

Gold nanorods (GNRs) have been researched extensively over the past decade, with emerging applications in therapeutics and diagnostics because of advantages associated with their anisotropic nature.<sup>[1]</sup> This shape confers specific optical properties, displaying two separate localized surface plasmon resonances in the visible and near-IR spectral range, because of the transverse (TSP) and longitudinal surface plasmons (LSP), respectively. However, to form the rods a concentrated solution of the surfactant cetyl trimethylammonium bromide (CTAB) is needed.<sup>[2]</sup> This is bound to the surface as a bilayer structure, which is difficult to remove and highly cytotoxic, thus limiting many potential biomedical applications.<sup>[3,4]</sup> A major challenge with replacement of CTAB by thiolated ligands is the destabilization of the protective CTAB bilayer upon initial functionalization leading to aggregation.<sup>[5,6]</sup>

There have been numerous approaches developed to overcome this problem and functionalize GNRs, such as round-trip phase transfer, strict control over sonication and temperature or ionic exchange resins.<sup>[5,7,8]</sup> Recently, the use of small thiolated ligands analogous to CTAB has been shown to undergo quantitative exchange on GNRs, however this is not applicable for less dense coatings where polymers are concerned.<sup>[9]</sup> Furthermore, we found procedures for functionalization with polymeric ligands to be ineffective at maintaining complete colloidal control. The uncertainty associated with a number of these methods would then lead to potentially inaccurate conclusions being drawn from in vitro and in vivo experiments when contemplating the GNR–cell interaction.

Towards the goal of a simple, biologically relevant, and robust functionalization procedure for GNRs, three necessary stages were identified. First, the excess CTAB in solution must be at the minimum possible concentration while maintaining colloidal stability. Second, the CTAB is desorbed in a controlled manner through addition of a solvent, such as ethanol. Third, the removal of CTAB is balanced by the concurrent addition of a stabilizing ligand such as thiolated polyethylene glycol (PEG). This resulted in a two-step functionalization protocol—a primary functionalization in water to confer stability with a second functionalization step in ethanol to completely detoxify the GNRs. A lower cytotoxicity and pro-inflammatory response was found for these rods versus those following a simpler one-step functionalization route.<sup>[10]</sup>

Experimentally, the GNRs were prepared following the seed-mediated growth in the presence of CTAB (see the

Supporting Information). Because of the dynamic equilibrium of CTAB between surface-adsorbed and bulk monomeric species in solution, the surfactant concentration was altered through centrifugation and dilutions. The PEGylation was performed over 24 h at RT, allowing an equilibrium to be reached and to aid comparisons with previous studies, while avoiding any effects of lateral diffusion of the thiolated PEG.<sup>[11]</sup>

To efficiently exchange the CTAB from the surface of the GNRs, we observed that it is helpful to first minimize the concentration of CTAB in the bulk to near the critical micelle concentration (cmc). The equilibrium formed with monomers in solution means that at this minimum concentration the CTAB bilayer on the sides of the rods is least stable. The GNRs were stable, here defined as no change within experimental error of the full width at half maximum (FWHM) of the LSP absorbance peak over a period of 5 days, down to a concentration of 1 mM (Figure 1). As

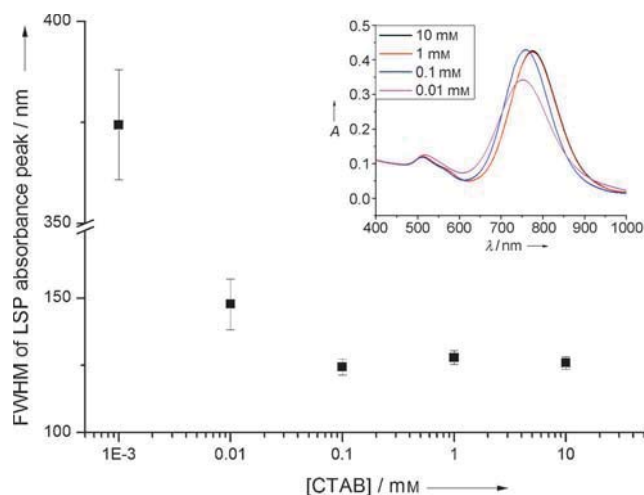


**Figure 1.** FWHM of the LSP absorbance peak against the concentration of the stabilizing surfactant, CTAB. Inset: corresponding spectra of GNRs at different concentrations of CTAB.

expected, this is close to the cmc of CTAB (0.8 mM) below which it is more energetically favorable for the surfactant to exist as monomers rather than self-assembled structures, such as the bilayer on the surface of the GNRs.<sup>[12]</sup> The GNRs were also metastable at 0.1 mM, with little change in the FWHM, although a blue shift of up to 5 nm was observed indicating a small degree of aggregation. These observations are consistent with those of Rostro–Kohanloo et al., where the ratio of CTAB to GNRs was found to be more crucial than the absolute concentrations of CTAB.<sup>[13]</sup> We chose to maintain a high ratio of CTAB to GNR, around  $1.4 \times 10^7$ , so the amount of CTAB on the surface can be considered negligible in comparison to the concentration in bulk.

Next, desorption of the remaining CTAB was controlled by addition of ethanol. After dilution and washing by centrifugation, the concentration of the GNRs and CTAB was 0.07 mM and 1 mM, respectively. The rods were stable up

[\*] C. Kinnear, Dr. H. Dietsch, Dr. M. J. D. Clift, C. Endes, Prof. B. Rothen-Rutishauser, Prof. A. Petri-Fink Adolphe Merkle Institute, University of Fribourg 1723 Marly (Switzerland) E-mail: alke.fink@unifr.ch Prof. A. Petri-Fink Department of Chemistry, University of Fribourg 1700 Fribourg (Switzerland)

[\*\*] This work was supported by the Swiss National Science Foundation (grant number PP00P2\_123373), the Adolphe Merkle Foundation, the Chemistry Department of the University of Fribourg and FriMat.

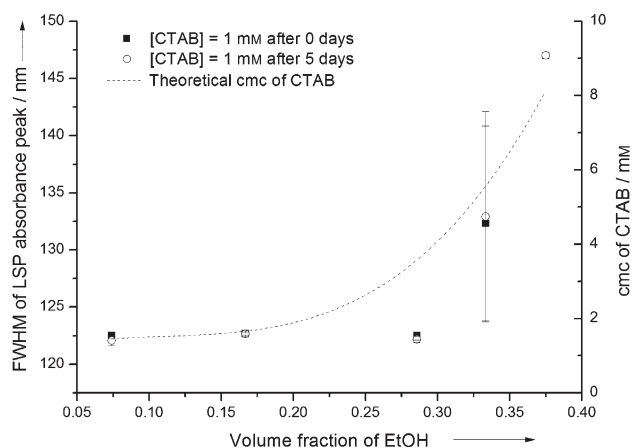


**Figure 2.** Decrease in the stability of GNR-CTAB, measured by the broadening of the LSP absorbance upon addition of ethanol. The theoretical cmc was fitted to literature data.<sup>[14]</sup>

to volume fractions of 0.30 after which point irreversible aggregation occurred for all volume fractions (Figure 2). The aggregation is due to the drastic lowering of the cmc by ethanol, which results in a destabilization of the bilayer on the surface of the GNRs. From the literature, a substantial change in the cmc occurs above ethanol volume fractions of 0.2–0.3, consistent with the point at which the GNRs destabilize (Figure 2).<sup>[14,15]</sup>

One of the most common methods to detoxify GNRs and increase circulation time is through grafting with PEG. This polymer is typically chemisorbed, to the surface through a terminal functional group. The coating imparts a stealth characteristic to the nanoparticle, leading to low levels of opsonization with plasma proteins and consequently low levels of uptake and clearance by macrophages.<sup>[16]</sup> In a typical experiment, the PEG was added to the GNRs in aqueous conditions ( $[CTAB] = 1 \text{ mM}$  and  $[NRs] = 0.6 \text{ nM}$ ) and left to react for 24 h at RT. Excess unreacted PEG was removed by centrifugation with the pellets re-dispersed in mixtures of ethanol and water. The stability of the rods was followed by the shifts in the LSP by UV/Vis spectroscopy and the hydrodynamic radius by dynamic light scattering (DLS) after addition of ethanol. However, we found that UV/Vis spectroscopy is more sensitive compared to DLS, because of the uncertainty in the local viscosity of the ethanol/water mixture, as well as domination of the faster rotational diffusion compared to the translational diffusion at scattering angles at or above  $90^\circ$ . At lower angles the presence of surfactant and ethanol in our system induces transient bubble formation—making any measurement challenging as highlighted by others.<sup>[17]</sup>

At low concentrations of PEG ( $\leq 5$  molecules of PEG  $\text{nm}^{-2}$ ) the GNRs are unstable at ethanol volume fractions above 0.30, determined by UV/Vis spectroscopy, most likely because of incomplete functionalization (Figure 3a). We recommend a minimum concentration of  $10 \text{ PEG nm}^{-2}$  for stabilizing the rods, qualitatively confirmed with DLS measurements. Previous findings indicate a maximum grafting density of PEG to spherical particles of  $1.6 \text{ PEG nm}^{-2}$ , however only  $0.052 \text{ PEG nm}^{-2}$  was found for CTAB-capped

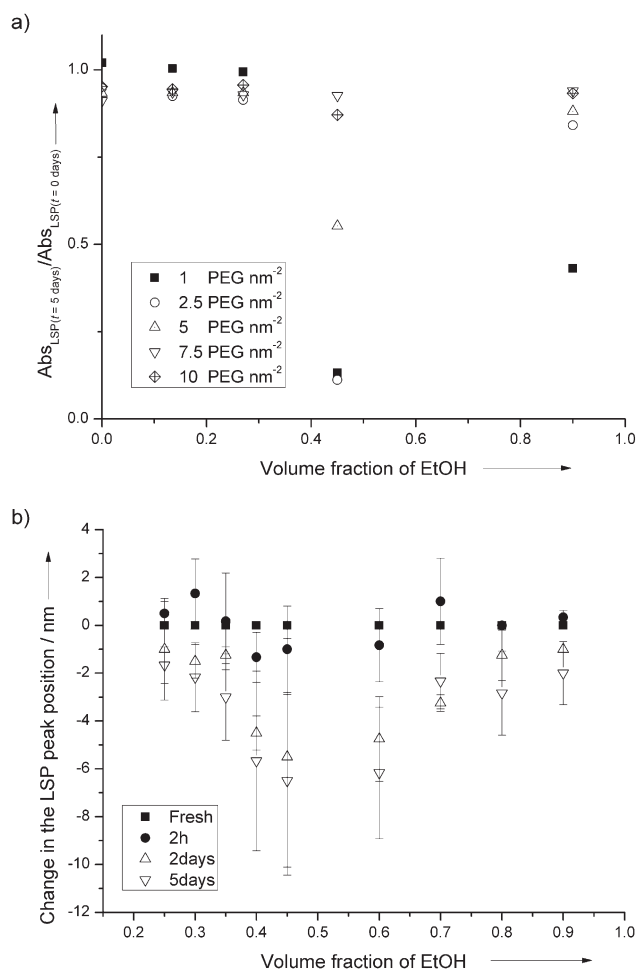


**Figure 3.** a) Impact of the PEG concentration on the GNR stability against volume fraction of ethanol, indicated by the ratio of absolute absorbance of the LSP absorbance after five days to the original value (error bars omitted for clarity, relative standard deviation, (RSD) = 9.2%). b) Shift in the position of the LSP peak relative to the fresh sample with time of a PEGylated GNR suspension. The rods were functionalized with PEG at a concentration of  $5 \text{ PEG nm}^{-2}$  and dispersed in binary mixtures of EtOH in water. The error bars represent standard deviation from three replicates.

GNRs confirming the need for excess PEG to fully functionalize the GNRs.<sup>[18]</sup>

These observations were further investigated. The concentration of PEG was chosen to infer partial stability to the GNRs ( $5 \text{ PEG nm}^{-2}$ ) and a shift in the LSP followed (Figure 3b). The shift was smallest for high and low concentrations of ethanol, whereas a sizable blue shift was found at intermediate concentrations. This is known to originate from side-on aggregation, where end-on-end aggregation would cause a red-shift.<sup>[19,20]</sup> These observations cannot be explained by the increased viscosity or refractive index of the binary ethanol/water mixture, and we rule out any reshaping of the GNRs as an increase in the hydrodynamic radius is concurrently observed. One possible origin of this is the end-functionalization with PEG, whereas the longitudinal side is, at least partially, coated with CTAB, observed by a number of other groups.<sup>[20,21]</sup> The destabilization at intermediate con-

concentrations of ethanol, and low concentrations of PEG, is understood through consideration of the hydrophobicity of surface-adsorbed CTAB. At low concentrations of ethanol, a bilayer is present. Increasing the ethanol content solubilizes more CTAB resulting in a single hydrophobic layer and destabilizing the GNRs. As the ethanol content is increased further the hydrophobic CTAB extending from the GNR surface is more stable and combined with the effect of PEG results in stable GNRs.

A total of 50 separate experiments were undertaken to map out the stability for GNRs as a function of the polymer and ethanol concentrations while keeping the concentration of CTAB constant at 1 mM. We generated a normalized stability parameter defined as the ratio of absolute absorbance to the original value before addition of ethanol. Visualizing this allows us to identify the region of instability to avoid when PEGylating GNRs and the concentrations where pronounced functionalization of the ends likely occurs (up to  $10 \text{ PEG nm}^{-2}$ ) after which there is partial exchange on the longitudinal sides (Figure 4). It should be noted that there is no accounting for statistical deviations in this map, as it is intended as a guide for PEGylation of GNRs. This variation is the reason for the region of lighter blue for GNRs functionalized with  $10 \text{ PEG nm}^{-1}$ .

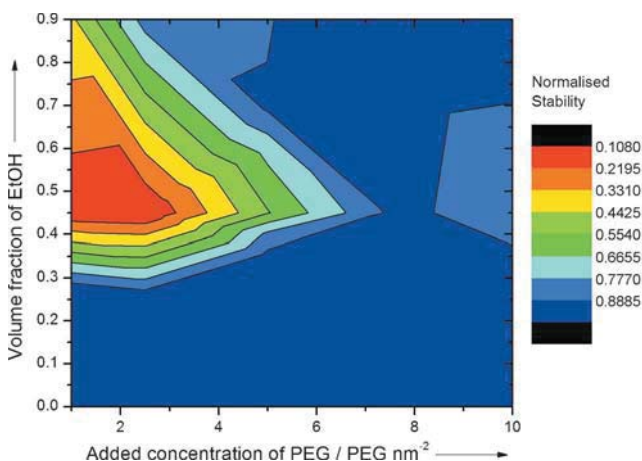


**Figure 4.** Phase diagram for the stability of the GNRs, where the normalized stability is the ratio of intensity of the LSP peak after five days relative to the initial value. A total of 50 evenly distributed data points corresponding to individual experiments contribute to this figure. PEGylation occurred over 24 h with  $[\text{CTAB}] = 1 \text{ mM}$ .

It has been shown that both surface-adsorbed CTAB and monomers in solution are responsible for cytotoxicity observed with GNRs; therefore it is desirable to remove the majority of surfactants before their use in any biological study. This is often difficult to confirm and indirect qualitative methods are used such as the decrease in the zeta-potential; or the disappearance of vibrational peaks in Fourier transform infrared spectroscopy (FT-IR).<sup>[7,22]</sup> Adding a huge excess of PEG to the CTAB-GNRs will result in a decrease in the zeta-potential and the near disappearance of the vibrational stretch of the quaternary amine, at  $958 \text{ cm}^{-1}$ , in the FT-IR spectra, however is this sufficient?

Employing the desorbing effect of ethanol, it is possible to further remove any bound CTAB which is not detected by zeta-potential measurements or FT-IR spectroscopy. Therefore, a comparison of functionalization strategies was made between PEGylated gold nanospheres, GNRs functionalized with excess PEG in a traditional one-step method ( $100 \text{ PEG nm}^{-2}$ ), and GNRs functionalized by the here described two-step procedure through ethanol washing. Gold nanospheres were chosen as the negative control because of their biocompatibility.<sup>[23]</sup> For the two-step method, the GNRs were functionalized with enough PEG for stabilization ( $10 \text{ PEG nm}^{-2}$ ) before a second functionalization step in ethanol ( $10 \text{ PEG nm}^{-2}$ , 90% v/v of ethanol in

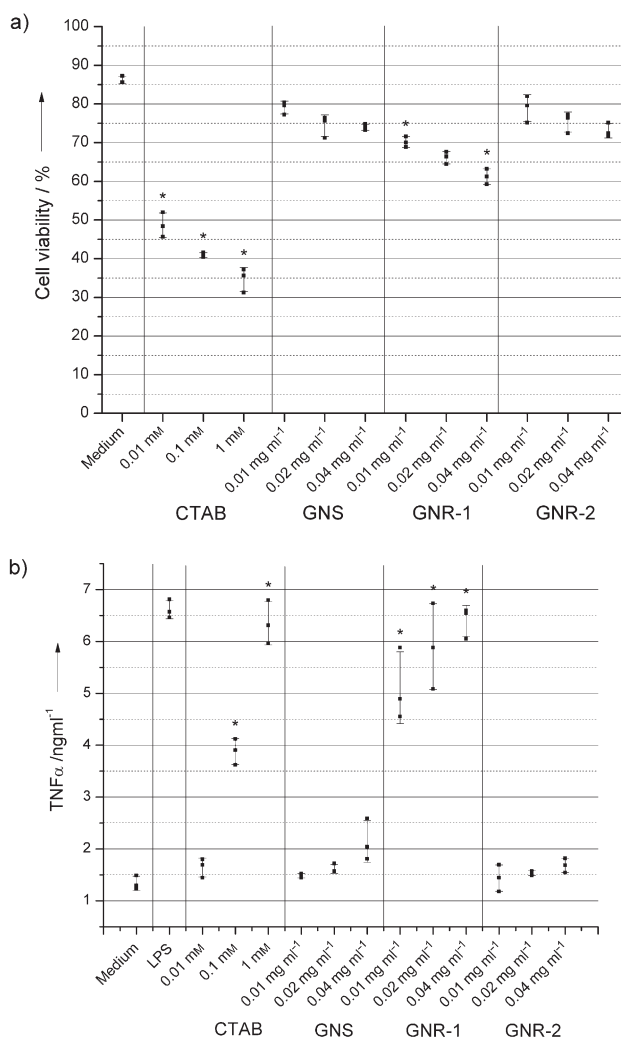


**Figure 5.** a) Human blood monocyte-derived macrophage (MDM) viability determined by the Trypan blue assay and b) release of pro-inflammatory cytokine tumor necrosis factor ( $\text{TNF-}\alpha$ ) from MDM after 24 h suspension exposure (lipopolysaccharide (LPS) was used as the positive control,  $0.1 \text{ mg mL}^{-1}$ ) to CTAB ( $0.01\text{--}1 \text{ mM}$ ), as well as PEGylated gold nanospheres (GNS), GNRs functionalized by a one-step method with excess PEG (GNR1), and GNRs functionalized by a two-step method with PEG through ethanol washing (GNR2;  $0.01\text{--}0.04 \text{ mg mL}^{-1}$ ). Bars denote the mean standard deviation. A pairwise t-test was performed and significance was indicated by:  $*p < 0.05$  versus a) GNS and b) medium.

water). Cell viability in primary human blood monocyte-derived macrophages was assessed by the Trypan blue assay and the release of the pro-inflammatory cytokine tumor necrosis factor- $\alpha$  (TNF- $\alpha$ ) was studied by an enzyme-linked immunosorbent assay (ELISA).<sup>[24]</sup> Despite the five-fold reduction in the quantity of PEG, the two-step method produced GNRs with the same cytotoxic and pro-inflammatory profile as gold nanospheres whereas the one-step GNRs were significantly more biologically adverse. These GNRs induced a significant reduction in the cell viability, as well as a highly significant increase in the inflammatory response observed by the elevated levels of TNF- $\alpha$ —on a similar level to the positive control (Figure 5). Both methods produced GNRs stable in ethanol, with no detectable CTAB by zeta-potential measurements or FT-IR spectroscopy. Nevertheless, an additional solubilization step with ethanol was crucial in reducing the biological impact of the GNRs.

The PEG attached after a two-step method was quantified by thermogravimetric analysis, and a grafting density of 0.89 PEG nm<sup>-2</sup> was found (see the Supporting Information). This is between that for a PEG “brush” on a nanosphere and a flat surface, as expected for GNRs.<sup>[18,25]</sup> Furthermore, <sup>1</sup>H NMR spectroscopy indicated that a small quantity of CTAB remained (see the Supporting Information)—most likely interchelated into the PEG brush because of the known interactions of PEG with surfactants.<sup>[26]</sup>

We have also applied this method successfully to PEG with functionalized end groups, which can undergo conjugation chemistry to attach desired tags, proteins, or targeting ligands while avoiding any unintended adverse biological effects from CTAB.

In conclusion, the exchange of PEG with CTAB on the surface of GNRs was studied as a function of the concentrations of polymer and ethanol, where a window of stability was identified for functionalization. As opposed to the standard PEGylation procedure of mixing in water, we found that enhanced exchange and stabilization of the GNRs occurred when ethanol was used to desorb the CTAB from the surface. Balancing the removal of CTAB with ethanol and the attachment of PEG whilst maintaining colloidal stability was found to be enhanced through a two-step functionalization protocol. This protocol allows complete functionalization of the GNRs with compatible ligands for use in biological systems, bringing reliability with regards to the exact nature of the surface ligands.

- 
- [1] a) P. K. Jain, K. S. Lee, I. H. El-Sayed, M. A. El-Sayed, *J. Phys. Chem. B* **2006**, *110*, 7238–7248; b) C. J. Murphy, T. K. Sau, A. M. Gole, C. J. Orendorff, J. Gao, L. Gou, S. E. Hunyadi, T. Li, *J. Phys. Chem. B* **2005**, *109*, 13857–13870.  
 [2] B. Nikoobakht, M. A. El-Sayed, *Chem. Mater.* **2003**, *15*, 1957–1962.

- [3] A. P. Leonov, J. Zheng, J. D. Clogston, S. T. Stern, A. K. Patri, A. Wei, *ACS Nano* **2008**, *2*, 2481–2488.  
 [4] a) A. M. Alkilany, P. K. Nagaria, C. R. Hexel, T. J. Shaw, C. J. Murphy, M. D. Wyatt, *Small* **2009**, *5*, 701–708; b) L. Vigderman, B. P. Khanal, E. R. Zubarev, *Adv. Mater.* **2012**, *24*, 4811–4841.  
 [5] B. Thierry, J. Ng, T. Krieg, H. J. Griesser, *Chem. Commun.* **2009**, 1724.  
 [6] B. P. Khanal, E. R. Zubarev, *Angew. Chem.* **2007**, *119*, 2245–2248; *Angew. Chem. Int. Ed.* **2007**, *46*, 2195–2198.  
 [7] A. Wijaya, K. Hamad-Schifferli, *Langmuir* **2008**, *24*, 9966–9969.  
 [8] Q. Dai, J. Coutts, J. Zou, Q. Huo, *Chem. Commun.* **2008**, 2858.  
 [9] L. Vigderman, P. Manna, E. R. Zubarev, *Angew. Chem.* **2012**, *124*, 660–665; *Angew. Chem. Int. Ed.* **2012**, *51*, 636–641.  
 [10] a) H. Liao, J. H. Hafner, *Chem. Mater.* **2005**, *17*, 4636–4641; b) Y. Qiu, Y. Liu, L. Wang, L. Xu, R. Bai, Y. Ji, X. Wu, Y. Zhao, Y. Li, C. Chen, *Biomaterials* **2010**, *31*, 7606–7619; c) A. S. Karakoti, S. Das, S. Thevuthasan, S. Seal, *Angew. Chem.* **2011**, *123*, 2024–2040; *Angew. Chem. Int. Ed.* **2011**, *50*, 1980–1994; d) N. M. Schaeublin, L. K. Braydich-Stolle, E. I. Maurer, K. Park, R. I. MacCuspie, A. R. M. N. Afroz, R. A. Vaia, N. B. Saleh, S. M. Hussain, *Langmuir* **2012**, *28*, 3248–3258; e) X. Huang, X. Peng, Y. Wang, Y. Wang, D. M. Shin, M. A. El-Sayed, S. Nie, *ACS Nano* **2010**, *4*, 5887–5896.  
 [11] a) M. J. Hostetler, A. C. Templeton, R. W. Murray, *Langmuir* **1999**, *15*, 3782–3789; b) P. Ionita, A. Volkov, G. Jeschke, V. Chechik, *Anal. Chem.* **2008**, *80*, 95–106.  
 [12] S. P. Moulik, M. E. Haque, P. K. Jana, A. R. Das, *J. Phys. Chem.* **1996**, *100*, 701–708.  
 [13] B. C. Rostro-Kohanloo, L. R. Bickford, C. M. Payne, E. S. Day, L. J. E. Anderson, M. Zhong, S. Lee, K. M. Mayer, T. Zal, L. Adam et al., *Nanotechnology* **2009**, *20*, 434005.  
 [14] W. Li, M. Zhang, J. Zhang, Y. Han, *Front. Chem. China* **2006**, *1*, 438–442.  
 [15] H. Akbaş, Ç. Kartal, *Colloid J.* **2006**, *68*, 125–130.  
 [16] D. E. O. Owens III, N. A. Peppas, *Int. J. Pharm.* **2006**, *307*, 93–102.  
 [17] M. Glidden, M. Muschol, *J. Phys. Chem. C* **2012**, *116*, 8128–8137.  
 [18] X. Xia, M. Yang, Y. Wang, Y. Zheng, Q. Li, J. Chen, Y. Xia, *ACS Nano* **2012**, *6*, 512–522.  
 [19] C. Tabor, D. van Haute, M. A. El-Sayed, *ACS Nano* **2009**, *3*, 3670–3678.  
 [20] A. Lee, A. Ahmed, D. P. dos Santos, N. Coombs, J. I. Park, R. Gordon, A. G. Brolo, E. Kumacheva, *J. Phys. Chem. C* **2012**, *116*, 5538–5545.  
 [21] a) L. Wang, Y. Zhu, L. Xu, W. Chen, H. Kuang, L. Liu, A. Agarwal, C. Xu, N. A. Kotov, *Angew. Chem.* **2010**, *122*, 5604–5607; *Angew. Chem. Int. Ed.* **2010**, *49*, 5472–5475; b) Z. Nie, D. Fava, E. Kumacheva, S. Zou, G. C. Walker, M. Rubinstein, *Nat. Mater.* **2007**, *6*, 609–614.  
 [22] T. Niidome, M. Yamagata, Y. Okamoto, Y. Akiyama, H. Takahashi, T. Kawano, Y. Katayama, Y. Niidome, *J. Controlled Release* **2006**, *114*, 343–347.  
 [23] a) C. Brandenberger, B. Rothen-Rutishauser, C. Mühlfeld, O. Schmid, G. Ferron, K. Maier, P. Gehr, A.-G. Lenz, *Toxicol. Appl. Pharmacol.* **2010**, *242*, 56–65; b) C. Brandenberger, B. Rothen-Rutishauser, F. Blank, P. Gehr, C. Mühlfeld, *Respir. Res.* **2009**, *10*, 22.  
 [24] M. J. D. Clift, P. Gehr, B. Rothen-Rutishauser, *Arch. Toxicol.* **2011**, *85*, 723–731.  
 [25] L. D. Unsworth, Z. Tun, H. Sheardown, J. L. Brash, *J. Colloid Interface Sci.* **2005**, *281*, 112.  
 [26] a) Z. Matras, T. Malcher, B. Gzyl-Malcher, *Thin Solid Films* **2008**, *516*, 8848; b) L. G. Qiu, M. J. Cheng, A. J. Xie, Y. H. Shen, *J. Colloid Interface Sci.* **2004**, *278*, 40.